

# Compact Zernike phase contrast x-ray microscopy using a single-element optic

O. von Hofsten,\* M. Bertilson, M. Lindblom, A. Holmberg, and U. Vogt

Biomedical & X-ray Physics, Department of Applied Physics, Royal Institute of Technology, Albanova, SE-10691 Stockholm, Sweden

\*Corresponding author: olov.hofsten@biox.kth.se

Received December 20, 2007; accepted March 14, 2008;  
posted March 25, 2008 (Doc. ID 93448); published April 23, 2008

We demonstrate Zernike phase contrast in a compact soft x-ray microscope using a single-element optic. The optic is a combined imaging zone plate and a Zernike phase plate and does not require any additional alignment or components. Contrast is increased and inverted in an image of a test object using the Zernike zone plate. This type of optic may be implemented into any existing x-ray microscope where phase contrast is of interest. © 2008 Optical Society of America  
OCIS codes: 340.0340, 340.7460.

High-resolution x-ray microscopy is a well-established imaging technique. Since the refractive index at x-ray wavelengths is close to one, radial diffractive gratings, also known as Fresnel zone plates, are commonly used as microscope objectives, and up to 15 nm resolution can be achieved [1]. When using soft x-rays in the so-called water window (2.3–4.4 nm), wet samples up to 10  $\mu\text{m}$  in thickness can be imaged owing to a natural absorption contrast between carbon and water, suiting applications in, e.g., biology [2] and soil science [3]. Beside synchrotron storage rings, which are most often used as sources, other compact laboratory-based sources exist for x-ray microscopy. Here, laser-produced plasmas generate the x-ray radiation that makes the arrangement fit on an optical table [4]. In this Letter we present the implementation of Zernike phase contrast in a compact soft x-ray microscope using a single optical element.

Absorption in the water window yields good image contrast between carbon and water. However, the primary result when x-rays interact with matter at this wavelength range is the phase shift of the radiation. This is clear when studying the complex index of refraction for x-ray wavelengths, given by  $n = 1 - \delta + i\beta$ . The  $\delta$  describes the phase shift introduced by the object, and  $\beta$  describes any absorption. The ratio of  $\delta$  and  $\beta$  is larger than 1 in the entire water window, indicating that contrast in soft x-ray microscopy would benefit from using this phase shift in phase contrast imaging. In fact, calculations have shown that the dose can be reduced by nearly a factor of 10 [5,6] when using phase contrast.

Two phase contrast techniques exist so far for high-resolution x-ray microscopy: differential-interference contrast (DIC) and Zernike phase contrast. DIC phase contrast was recently demonstrated in our compact soft x-ray microscope [7], but Zernike-type phase contrast has mostly been demonstrated at synchrotron-based microscopes, although in the hard x-ray regime there exists a commercial instrument using this technique [8]. It was first proven in the water window [9] and later at higher energies [10] with the principle being the same as in optical mi-

croscopy [11]. A phase-shifting annular ring is placed in the back focal plane of the objective, designed to match the undiffracted light from the condenser. Therefore the condenser area cannot be too large and is usually masked. Phase contrast is achieved as the undiffracted radiation from the object is phase shifted by the ring, enabling it to interfere with the diffracted radiation in the image plane.

Zernike-type phase contrast imaging is well suited for our compact soft x-ray microscope, since the required hollow cone illumination is provided by the condenser [4]. However, in the current arrangement, there is no possibility of incorporating such a phase-shifting ring without adding additional components to the microscope. Here we present Zernike phase contrast in a compact soft x-ray microscope using a single optical element where the annular phase-shifting ring has been incorporated into the zone plate, making alignment and implementation straightforward. This Zernike zone plate (ZZP) has

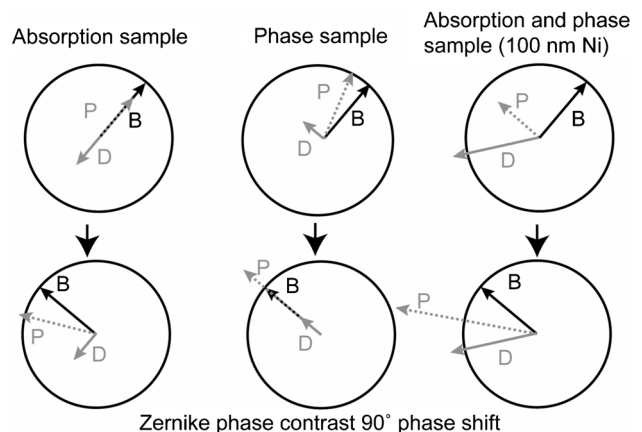


Fig. 1. Phasor diagrams of various samples and optics. (top) The situation when using a normal zone plate for three types of samples. (bottom) The same samples when using Zernike phase contrast. The contrast, i.e., the difference in magnitude between the particle ( $P$ ) wave and the background ( $B$ ), has changed in comparison with the diagrams above. The  $D$  wave is the diffracted wave, given by subtracting the  $B$  from the  $P$  wave.

been successfully tested in the microscope, and images show increased contrast owing to phase contrast. The technique is demonstrated here for soft x-ray microscopy but is also suitable for the hard x-ray regime, where the absorption in biological samples is small and phase contrast must be used.

When x-ray radiation interacts with an object, part of the radiation will pass straight through unaffected, while some will interact with the material and be diffracted and phase shifted. When there is absorption in the object, the undiffracted and the diffracted light will interfere in the image plane and give good contrast. When the object does not exhibit absorption, but merely a phase shift due to longer or shorter optical path length, phase contrast methods are preferred. Zernike phase contrast turns the phase information from the object into image intensity by phase shifting the undiffracted background relative to the diffracted wave. Following [10,12], the underlying theory can be understood by studying the phasor diagrams of the undiffracted background ( $B$ ), diffracted ( $D$ ), and resulting particle wave ( $P$ ), seen in Fig. 1.

For basic understanding, the first diagram (top left) shows a phasor diagram for an absorption sample, imaged by a regular optic. The background has been given an arbitrary phase and magnitude, and the particle wave has the same phase but a smaller magnitude. Since the particle wave is given by the interference between the  $B$  and  $D$  waves, it follows that  $P=B+D$ , so the  $D$  wave must be phase shifted by  $180^\circ$ . The next diagram (top center) shows the phasor diagram for a phase sample where the phase shift is much smaller than the wavelength. The particle wave has not been absorbed and thus has nearly the same amplitude as the  $B$  wave. The  $D$  wave is therefore phase shifted by approximately  $90^\circ$  in comparison with the background. The lower diagrams show the same type of samples as the upper diagrams, but here Zernike phase contrast has been used, where the  $B$  wave is phase shifted by  $90^\circ$ . This corresponds to positive phase contrast, where for x-rays the particle wave shows a higher intensity than the background.

The basic idea of the ZZZP is to replace the phase ring by phase-shifted zones on the zone plate itself. The phase-shifted zones are those that are directly illuminated by the condenser. This is possible if the illumination is spatially defined on the zone plate objective, as in the case of hollow-cone illumination. Figure 2 shows the illumination situation in our microscope, from which it is clear that the illumination from the condenser that is not affected by the object ( $B$  wave) will hit the phase-shifted zones on the ZZZP, whereas the diffracted radiation (illustrated by dark rays) is spread over the entire aperture. Figure 2 also shows that some of the diffracted light will be phase shifted by the ZZZP. The result will be halo effects in the image as well as shade-off artifacts that yield lower image intensity for large structures. These are well-known effects in visible light Zernike phase contrast microscopy [13]. The effects are considered both positive, since they actually can give an edge en-

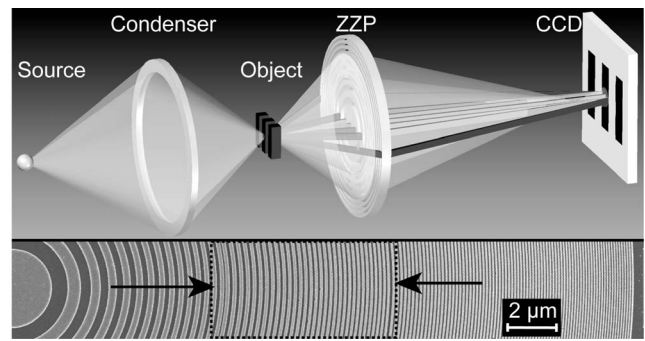


Fig. 2. (top) Illustration of the implementation of Zernike phase contrast in our microscope. The zones of the ZZZP that are directly illuminated by the condenser are phase shifted with respect to the rest of the optic. (bottom) Detail of SEM image of the ZZZP. The phase-shifted zones are marked by the dashed area and the arrows.

hancement, and negative, owing to the difficulties in interpreting an image with artifacts.

The experimental arrangement consists of a pulsed, frequency-doubled Nd:YAG laser focused on a  $20\ \mu\text{m}$  liquid-nitrogen jet producing a high-brightness soft x-ray plasma source. The characteristic emission spectrum of nitrogen is then filtered to a wavelength of  $2.48\ \text{nm}$ . The source is imaged by a condenser zone plate with an outermost zone width of  $49\ \text{nm}$  and a diameter of  $4.53\ \text{mm}$ , giving critical illumination. The condenser has a central stop to avoid stray light from the strong zeroth-order, which makes the condenser annular with a ring width of  $376\ \mu\text{m}$ . Therefore, the condenser ring is sufficiently small, and no masking is necessary. The ZZZP has an outermost zone width of  $50\ \text{nm}$  and a diameter of  $50\ \mu\text{m}$ , and the phase-shifted ring has an inner radius of  $8.5\ \mu\text{m}$  and a width of  $6.7\ \mu\text{m}$ . The width of the ring is therefore  $\sim 3$  times larger than the hollow cone illuminating the ZZZP, keeping realistic alignment margins. The regular zone plate is identical to the ZZZP except for the phase-shifted zones. However, one cannot rule out quality differences due to the fabrication process. The object imaged by the ZZZP is detected by a backilluminated CCD camera with a pixel size of  $13.5\ \mu\text{m}$ . More information about the compact soft x-ray microscope is given in [4].

The zone plates were manufactured using a three-layer process that is described in more detail elsewhere [14]. Calculations made with software developed to simulate the illumination in the microscope [15] show that positive phase contrast would yield the best results for the given sample, with the additional advantage of a clear result, since this gives an inverted contrast in the x-ray region. The zones are thus phase shifted by  $-90^\circ$ , which is equivalent to a translation toward the center of the zone plate by one-quarter period. A scanning electron microscopy (SEM) picture of the resulting zone plate is shown in Fig. 2, where the phase-shifted zones are outlined by a dashed box. The borders of the phase ring, shown with arrows in the figure, are seen as irregularities in the zone plate pattern.

Figure 3 shows images taken using a normal zone plate and with the ZZZP. The imaged object is a grat-

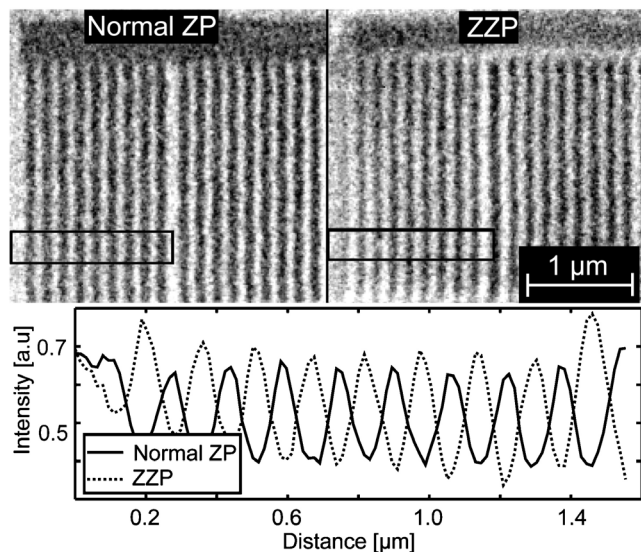


Fig. 3. Images of 80 nm nickel lines using a normal zone plate (top left) and using the Zernike zone plate (ZZP, top right). Image profiles are compared in the lower plot. The contrast is inverted and increased when using the ZZP.

ing with 80 nm lines of nickel, with a thickness of approximately 100 nm. The exposure time for both images was 6 min, and the magnification was 860.

As seen in Fig. 3, the contrast is indeed inverted in the image taken with the ZZP. In addition, the image contrast has increased from 20% to 25% on average, which is clear from the image profiles. The profiles are averaged over the area shown in the images. This area shows a strong contrast increase, while in other areas the effect is not as pronounced. The reason for this nonuniformity is provided below. Typical shade-off and halo artifacts are also seen in the image taken with the ZZP. Phasor diagrams for the two images are shown in the far right of Fig. 1. The nickel structures give a phase advance of approximately  $90^\circ$  in addition to absorption. When using a normal zone plate, the resulting contrast between the  $P$  and  $B$  wave is the same as for an absorption sample. When the ZZP is used, the image contrast is inverted and increased (lower right).

A disadvantage of moving the phase ring from the back focal plane of the zone plate to the zone plate itself is that the entire field of view will not show the phase contrast effect. Since the illumination in the zone plate plane is not as collimated as in the back focal plane, the phase-shifted ring will only phase shift undiffracted light coming from the center of the field of view. Outside of this area, the undiffracted light will only be partially phase shifted or miss the phase-shifted ring totally. Therefore, the phase contrast effect is most efficient within a  $5 \mu\text{m}$  diameter in the center of the field of view and decreases toward

the edges, as seen in the ZZP image. During alignment, this effect can be used as an accurate position of the ZZP with respect to the condenser. A slight misalignment or defocus will not give the phase-contrast effect in the center of the field of view but in some other area.

To conclude, we have achieved Zernike phase contrast x-ray microscopy in the water window yielding image contrast increase for the given nickel test sample. The single-element optic requires no extra alignment, and there is no observed reduction in resolution. This type of optic makes it possible for any existing soft x-ray microscope to use Zernike phase contrast, since no extra components are needed in the setup. The optic is not limited to soft x-ray microscopy but may also be incorporated into hard x-ray microscope setups.

*Note added in proof.* After the submission of this work, a publication by Sakdinawat and Liu [16] appeared where a similar optic was tested in a microscope using synchrotron radiation.

This work was funded by a grant from the Swedish Research Council.

## References

1. W. Chao, B. D. Harteneck, J. A. Liddle, E. H. Anderson, and D. T. Attwood, *Nature* **435**, 1210 (2005).
2. D. Weiss, G. Schneider, S. Vogt, P. Guttman, B. Niemann, D. Rudolph, and G. Schmahl, *Nucl. Instrum. Methods Phys. Res. A* **467**, 1308 (2001).
3. J. Thieme, G. Schmahl, D. Rudolph, and E. Umbach, eds., *X-Ray Microscopy and Spectroscopy* (Springer-Verlag, 1998).
4. P. A. C. Takman, H. Stollberg, G. A. Johansson, A. Holmberg, M. Lindblom, and H. M. Hertz, *J. Microsc.* **226**, 175 (2007).
5. J. Kirz, C. Jacobsen, and M. Howells, *Q. Rev. Biophys.* **28**, 33 (1995).
6. G. Schneider, *Ultramicroscopy* **75**, 85 (1998).
7. M. Bertilson, O. von Hofsten, M. Lindblom, T. Wilhein, H. M. Hertz, and U. Vogt, *Appl. Phys. Lett.* **92**, 064104 (2008).
8. XRadia Inc., <http://xradia.com/Products/nanoxct.html> (2008).
9. G. Schmahl, D. Rudolph, G. Schneider, P. Guttman, and B. Niemann, *Optik (Jena)* **97**, 181 (1994).
10. U. Neuhausler, G. Schneider, W. Ludwig, M. A. Meyer, E. Zschech, and D. Hambach, *J. Phys. D* **36**, 79 (2003).
11. F. Zernike, *Physica (Utrecht)* **9**, 686 (1942).
12. S. G. Lipson, H. Lipson, and D. S. Tannhauser, *Optical Physics* (Cambridge U. Press, 1995), pp. 348.
13. A. H. Bennett, H. Jupnik, H. Osterberg, and O. W. Richards, *Phase Microscopy*, (Wiley, 1951).
14. A. Holmberg, S. Rehbein, and H. M. Hertz, *Microelectron. Eng.* **73-74**, 639 (2004).
15. O. von Hofsten, P. A. C. Takman, and U. Vogt, *Ultramicroscopy* **107**, 604 (2007).
16. A. Sakdinawat and Y. Liu, *Opt. Express* **16**, 1559 (2008).